

## Studies of the Wall Shift in the Hydrogen Maser\*<sup>†</sup>

Paul W. Zitzewitz<sup>‡</sup> and Norman F. Ramsey

*Lyman Laboratory of Physics, Harvard University, Cambridge, Massachusetts 02138*

(Received 19 June 1970)

The frequency shift in the hydrogen maser caused by the collisions of the atoms with the storage bulb surface, usually called the wall shift, has been investigated as a function of temperature from 100 to 400 °K. The wall shift for Teflon, negative at room temperature, passes through zero as the temperature is raised above 380 °K. This constitutes the first observation of a positive wall shift. Below room temperature the shift becomes increasingly negative. Both the homopolymer polytetrafluoroethylene (Dupont TFE-42) and its copolymer with hexafluoropropylene (DuPont FEP-120) exhibit similar behavior. Changes in the shape of the temperature dependence have been found at temperatures where phase changes are known to occur in Teflon, connecting the wall shift directly to properties of the surface material. A theory is advanced which correctly predicts the wall shift at room temperature, but gives a temperature dependence much smaller than that found experimentally.

### I. INTRODUCTION

The hydrogen maser<sup>1,2</sup> is an active atomic oscillator which achieves its superb frequency stability and accuracy by storing the radiating atoms within regions of equal phase in a microwave cavity by means of a coated storage vessel. Although the vessel is the key to the maser's stability, it is the collisions of the atoms with the walls of this vessel which cause the perturbations to the free-space properties of the atoms that are most difficult to predict, to measure, and to control. The contribution of the collisions to the relaxation of the atomic spin polarization and phase coherence has been extensively investigated by Berg.<sup>3</sup> The present paper reports studies of the offset in the oscillation frequency caused by the surface collisions, the wall shift.

The oscillation frequency of a hydrogen maser differs from the free-space value of the hydrogen hyperfine frequency because of the effects of applied magnetic field, stimulating radiation field, collisions with other hydrogen atoms, atomic motion, and collisions with the storage bulb. The perturbation caused by the static magnetic field which is needed to provide an axis of quantization can be measured by determining the strength of the field by means of a double resonance experiment.<sup>1</sup> The hyperfine offset is then found through the Breit-Rabi formula. The frequency pulling caused by the mistuning of the microwave cavity can be adjusted to cancel the frequency shift caused by spin exchange during hydrogen-hydrogen collisions.<sup>4</sup> This is accomplished by varying the atomic linewidth and tuning the cavity to the point where oscillation frequency is independent of linewidth. The frequency shift due to the second-order Doppler effect (time dilatation), which is proportional to the average of

the square of the atomic velocity, can be obtained by measuring the temperature of the storage bulb with the assumption that the atoms, making nearly  $10^5$  collisions with the surface, are in thermal equilibrium with it.<sup>1</sup> Each of these frequency shifts can be measured to  $10^{-13}$  fractional accuracy in a few minutes of observation time.

The frequency shift due to surface collisions, on the other hand, involves a complex interaction of a hydrogen atom with a surface. With the lack of complete understanding of the hyperfine shift of a hydrogen atom in collisions with single helium atoms,<sup>5</sup> it is not surprising that the theory of the problem of collisions with a compound surface is rudimentary at best. Experimental determination of the wall shift in the past has been limited mainly to determinations of the size of the shift (fractionally about  $2 \times 10^{-11}$ ), and these have often differed widely.<sup>6</sup> The present series of experiments includes measurements of the shift due to several surface materials over a wide range of temperatures.<sup>7</sup> The results have helped to provide a choice between various theoretical models, as well as to suggest the direction of approach in the search for better surface materials.

In Sec. II the requirements of a surface are discussed and a theory of the wall shift is outlined. The shift of the hyperfine frequency of hydrogen due to a collision with a single atom is calculated, then the result is extended to a collision with a surface. Finally, an estimate of the amount of kinetic energy transferred during a collision is made. Section III describes the equipment and techniques, and Sec. IV the experimental results which are discussed in Sec. V. Section VI lists some additional experiments carried out, and Sec. VII offers some conclusions.

## II. WALL-SHIFT THEORY

### A. Surface Characteristics

There are some general requirements for a surface suitable for the storage bulb in the hydrogen maser. Primarily the surface must inhibit hydrogen recombination as well as preserve spin alignment and phase coherence over many collisions. Since atomic hydrogen is extremely reactive, it is essential that the surface be very inert so that the combined hydrogen-surface forces are weak enough to prevent atoms from sticking to the surface, thus providing sites for hydrogen recombination.<sup>3</sup> In addition, the bonds within the surface material must be strong enough to resist attack by the hydrogen atoms. Surfaces must also be nonconducting to avoid disturbing the microwave cavity. These properties are all fulfilled by a material which is made up of electronically saturated atoms joined by single covalent bonds. Multiple bonding should be avoided because atomic hydrogen can easily break this type of bond. Later discussion will show that it is important that the atoms have a low electric polarizability. With a surface of neutral atoms the lowest-order long-range force between them and the colliding hydrogen atoms is the van der Waals force, or induced dipole-induced dipole (dispersion) interaction. A surface with fixed dipole moments is not excluded from consideration because the dipole-induced dipole interaction is usually no larger than the van der Waals contribution.

The most commonly used surfaces in masers are the saturated hydrocarbons and their halogen analogs. Among the hydrocarbons both paraffin waxes and Drifilm (dimethyldichlorosilane) have been used. Both are satisfactory, but cause excessive spin and phase relaxation due to spin exchange between gaseous and surface hydrogen atoms.<sup>3</sup>

The halogen analogs of these substances, and especially the fluorocarbons with their low polarizabilities, offer significant advantages. The first is the lack of hydrogen-hydrogen spin exchange.<sup>8</sup> The second is the reduction in the atom-surface interaction made possible by the physical and chemical properties of the fluorine atoms. Because of their size and great electron affinity, they form an excellent protective sheath about the carbon core, giving the saturated fluorocarbons "a backbone of diamond and a skin of rhinoceros hide."<sup>9</sup>

For a practical coating it must be possible to make the material as a film that can be coated on a rigid bulb. At very low temperatures almost any material can be made to condense on the surface as a film. At room temperatures some experiments have been done with a liquid fluorocarbon, as will be discussed later. Some solid fluorocarbon waxes with molecular weights around  $10^4$  g/mole have the required vapor pressure (under  $10^{-6}$  Torr) to avoid excessive

gas phase collisions, but it has been found difficult to form surface films with them. The most successful coatings found so far have been various forms of Teflon.

Teflon is a synthetic polymerized fluorocarbon.<sup>10</sup> The homopolymer polytetrafluoroethylene has a chemical composition  $X(\text{CF}_2)_n X$  (where  $X$  stands for either F or an impurity end atom), with the molecular structure a long linear chain. Average molecular weight is from  $10^5$  to  $10^7$  g/mole. Teflon is also available as a copolymer of tetrafluoroethylene and hexafluoropropylene, where typically 5% of the  $(\text{CF}_2\text{CF}_2)$  monomers are replaced by  $(\text{CF}_2\text{CF}(\text{CF}_3))$  comonomers. There is no theoretical or experimental indication that these molecular chains are not also linear. The molecular weight is typically  $10^5$  g/mole.

The most widely accepted model for the structure of the Teflon solid is that of a semicrystallized form with lamellar crystals.<sup>11,12</sup> The long molecular chains are folded back and forth on themselves into a flat broad crystal with chains mainly perpendicular to the faces. Most of the disordered chains are on the crystal faces, but there is no general agreement on this point. The differences between homopolymer and copolymer structures are mainly the reduced amounts of crystal order and lamellar thickness in the latter.

Commercial Teflon products used in the maser are purchased as water-based dispersions of highly crystallized particles about  $1 \mu\text{m}$  across. The homopolymer product used is DuPont TFE-42, having 35% solids and a molecular weight of several million. The copolymer is DuPont FEP-120, 54% solids and a molecular weight about one-tenth of the homopolymer. A wetting agent is included in the copolymer and must be added to the homopolymer, as will be discussed below. Coating techniques, reviewed elsewhere,<sup>13,14</sup> produce a solid film about  $10^{-2}$  cm thick. The TFE-42 films are slightly milky white while the FEP-120 films are clear.

Although impurity levels in these proprietary commercial substances are difficult to ascertain, it is known that for a polymer synthesized by addition, that is, by adding monomers one by one to the end of a polymer chain, the resultant ends are most likely to contain impurities. It is a matter of fair agreement that both ends of the chains contain impurities of the type  $\text{CF}_2\text{H}$ .<sup>15,16</sup> It is also likely that these end groups are on the surfaces of the crystals,<sup>17</sup> and thus directly exposed to the hydrogen atoms in the maser. In order to reduce impurities then, it is best to use as high a molecular weight substance as possible.

The wetting agent used in both Teflon forms, Triton X-100 (Rohm and Haas), is required to allow the formation of the films and their adherence to the quartz bulb. It may introduce other impurities,

although all but trace amounts should be oxidized during the coating process.<sup>18</sup>

### B. Hyperfine Shift Theory

The hyperfine energy separation in the ground state of hydrogen is given, in the Fermi approximation,<sup>19</sup> by

$$E_h = \frac{8}{3} \pi g_i g_j \mu_B \mu_N m_i m_j |\Psi_1(0)|^2, \quad (1)$$

where  $\Psi_1(0)$  is the ground-state electronic wave function evaluated at the nucleus and other symbols have their usual meaning. When the atom is far from the surface, the attractive forces decrease the density of the wave function at the nucleus, lowering the hyperfine energy. When the direction of motion of the atom is reversed by the overlap of the electron clouds of the atom and surface, the wave function at the origin is increased, raising the hyperfine energy. A similar interaction leads to the pressure shifts observed in optical pumping experiments with buffer gases. Each surface collision shifts the phase of the oscillating hyperfine moment by the amount

$$\phi = \hbar^{-1} \int_{\Delta\tau} dt \delta E_h(t), \quad (2)$$

where  $\Delta\tau$  is the duration of the collision and  $\delta E_h(t)$  is the shift of the hyperfine energy.

To evaluate this integral, the variable  $t$  is replaced by the distance of the atom from the surface  $z$ , divided by the component of velocity perpendicular to the surface  $v_\perp$ . With the assumption that the surface is smooth, the component of momentum parallel to the surface is conserved during the collision, while the perpendicular component is affected by the atom-surface interaction. It is also assumed that energy is conserved during the collision, an assumption supported by calculations to be presented later. An atom with energy  $E$  approaching the surface at an angle  $\theta$  to the normal acquires a phase shift

$$\phi(E, \theta) = 2\hbar^{-1} \int_{z_0(E, \theta)}^{z_0(E, \theta)} dz \delta E_h(z) \times \left\{ \frac{2}{m} [E \cos^2 \theta - V(z)] \right\}^{-1/2}, \quad (3)$$

where  $m$  is the mass of the hydrogen atom,  $V(z)$  the atom-surface potential, and  $z_0$  the classical turning point. The net average phase shift per collision is an average of this shift over appropriate distributions in  $\theta$  and  $E$ .

$V(z)$  and  $\delta E_h(z)$  can be approximately generated by taking a suitable sum over potentials and energy shifts from individual two-body interactions between the hydrogen atom and surface atoms or groups of atoms. The constituent group of atoms in Teflon is  $\text{-CF-}$ , where the horizontal line (-) represents

the bonds to the adjacent groups. The concept of treating Teflon as an assembly of these units held together by covalent bonds along the molecular chains and by dipole-dipole and dispersion forces between chains has been explored previously.<sup>20</sup> This approach should be especially satisfactory in Teflon because the highly electronegative fluorine atoms prevent effective penetration of perturbing interactions beyond the fluorine sheath.<sup>9</sup> In the present problem the interactions in question are not between like groups of atoms, but between a hydrogen atom and a  $\text{-CF}_2\text{-}$  group.

Because of the complicated nature of this interaction an empirical potential, the Lennard-Jones (12, 6), has been used.<sup>21</sup> The problem at hand is to find the potential parameters<sup>21</sup>  $\epsilon$  and  $\sigma$  for the interaction between H and  $\text{CF}_2$  from H-H and  $\text{CF}_2\text{-CF}_2$  potentials. The normal technique is to use the arithmetic mean of the collision radii  $\sigma$  and the geometric mean of the attractive potential strengths  $C_- \equiv 4\epsilon\sigma^6$ . No attempt has been made to improve the first combination rule, but two alternative forms have been developed for the potential strength rule. These are based on the Slater-Kirkwood approximation for the strength of the dominant contribution to the attractive term in the Lennard-Jones potential, the lowest-order dispersion term,

$$C_6 = \frac{3}{2} \alpha_1 \alpha_2 [(\alpha_1/N_1)^{1/2} + (\alpha_2/N_2)^{1/2}]^{-1}, \quad (4)$$

where  $\alpha_1$  and  $\alpha_2$  are the static electric polarizabilities for the atoms and  $N_1$  and  $N_2$  adjustable parameters approximately equal to the number of electrons in the valence shell of the atoms. It has been shown<sup>22</sup> that by choosing  $N_1$  and  $N_2$  separately to make the Slater-Kirkwood  $C_6$  equal to more exact calculations of the interaction for pairs of like atoms,<sup>23</sup> the combined  $C_6$  is very close to the more exact value for the dissimilar pair. However, contributions from higher-order terms make  $C_- > C_6$ . This can be thought of as due either to an augmented polarizability or to a larger number of effective valence electrons. Thus two new combination rules for  $C_-$  are possible via the Slater-Kirkwood technique above. The final potential strength is taken as an arithmetic average of the three approximations.

The numerical values for the parameters in a. u. are for hydrogen,<sup>21</sup>  $\sigma = 1.469$ ,  $\alpha = 4.481$ ,  $C_- = 7.017$ ; for the  $\text{-CF}_2\text{-}$ ,<sup>20</sup>  $\sigma = 9.730$ ,  $\alpha = 13.90$ ,  $C_- = 265.6$ . The resultant parameters for H- $\text{CF}_2$  are  $\sigma = 5.6$  and  $\epsilon = 0.315 \times 10^{-3}$ , or  $\epsilon/k = 99.4^\circ \text{K}$ .

Calculations of the effect of intermolecular potentials on the hydrogen hyperfine energy have the same strengths and weaknesses as the calculations of the potentials themselves. Calculations of the effect of the dispersion force alone on the hyperfine energy of hydrogen have been carried out by the Das group<sup>5</sup> for the case of helium and neon, and for all noble gases by Davison.<sup>24</sup> They are in sub-

stantial agreement. Das has also calculated the effect of the repulsive potential, as has Clarke,<sup>25</sup> for the H-He interaction. Neither agrees with experiment.<sup>26</sup>

An approximate equation due to Adrian<sup>27</sup> relates the hyperfine shift to the dispersion interaction for any perturbing atom. He writes

$$\delta E_h/E_h = (-C_6 r^{-6}) [2I_h^{-1} + (I_h + I_a)^{-1}] , \quad (5)$$

where  $I_h$  and  $I_a$  are energies associated with the hydrogen and perturbing atoms, respectively. Comparison of this approximation with the more exact values for the rare gases<sup>24</sup> shows that the use of the ionization energies for all atoms yields agreement within a few percent. Substitution of the appropriate values for hydrogen and Teflon<sup>28</sup> gives

$$\frac{(-\delta E_h/E_h)}{(C_6 r^{-6})} \equiv R_0 = 4.9 \text{ a. u. .}$$

Because of the difficulty with the repulsive term and the resultant need to use an empirical potential to describe the interatomic interaction, the Adrian formula has been applied to the entire Lennard-Jones potential instead of just  $C_6$ . In order to separate the effects of the relatively well-understood long-range potential from those of the short-range forces, the hyperfine shift is divided into two parts,

$$\delta E_h = \delta E_h^{sr} + \delta E_h^{lr} ,$$

where

$$\begin{aligned} \delta E_h^{sr} &= E_h R_0 V^{sr} , & \delta E_h^{lr} &= E_h R_0 V^{lr} ; \\ V^{sr} &= 4\epsilon(\sigma/r)^{12} , & V^{lr} &= -4\epsilon(\sigma/r)^6 . \end{aligned}$$

These two-body interactions must now be extended to the atom-surface problem. The simplest method is to replace the point sources of the interaction with an equal number of sources spread homogeneously throughout the volume of surface material. This approach produces an analytical potential with power dependences reduced by three.<sup>29</sup> Thus,

$$\int dV N_3 C_n r^{-n} = 2\pi N_3 C_n (n-3)^{-1} (n-2)^{-1} z^{-(n-3)} ,$$

where  $N_3$  is the number of interaction centers per unit volume,  $z$  is the distance of the hydrogen atom above the surface, and the integral is taken over a semi-infinite volume. Thus the Lennard-Jones potential becomes

$$V = 4\epsilon(\pi/6)N_3\sigma^3 \left[ \frac{2}{15} (\sigma/z)^9 - (\sigma/z)^3 \right] . \quad (6)$$

Taking  $N_3$  from the density of polytetrafluoroethylene and the other parameters given above, the integrated potential gives a depth of 150 °K, an equilibrium separation 4.81  $a_0$ , and a zero crossing (collision radius) 4.00  $a_0$ .

It has been pointed out that this approximation underestimates the depth of the true potential ob-

tained by summing the two-body interactions over all surface atoms.<sup>29</sup> This is because the very strongly distance-dependent terms are weakened by the smearing of the force centers. One way to minimize this error without resorting to performing the complete summation is to replace the integral by a sum over a region around the immediate collision site and an integral over the remainder of the volume. This is especially appropriate in Teflon and other semicrystalline materials which have short-range order but long-range disorder. The structure of Teflon suggests that the most likely surface configuration of the molecular chains is a collection of folds. The tightest possible fold is a semicircle of diameter 0.566 nm, the interchain separation.<sup>10</sup> Seven  $-CF_2-$  groups fit on such a segment. Assuming the hydrogen atom is always directly above the  $-CF_2-$  group at the top of the fold, the sum over these seven groups is easy to find. It requires a numerical integration, however, to find the contribution to the integral from the semi-infinite volume minus the volume containing the summed fold. The final potential was found for many discrete values of  $z$ , and has a depth, using the parameters listed previously, of 225 °K, an equilibrium separation of 5.8  $a_0$ , and a zero crossing separation of 5.2  $a_0$ .

Two calculations of the phase shift per collision have been made. The first used the composite potential described above. An average over approach angles was made, assuming a distribution given by the cosine (Lambert) law, but no energy average was performed. Separation of the hyperfine shift into short- and long-range components was made and the results are shown in Fig. 1. The phase shifts are shown both as a function of approach angle at 300 °K and for the averaged angles from 50 to 400 °K.  $\epsilon_0$  is the potential depth listed above, and the results for  $3\epsilon_0$  and  $\frac{1}{3}\epsilon_0$  show the dependence of the results on different potential depths. It is clear that all temperature and angular dependence comes from the long-range contribution. This is purely kinematic in origin; the atom spends more time crossing the negative phase-shift region when it is going slower or at a more grazing angle. It should be noted that the more obvious nonkinematic corrections, for instance, from the dependence of Teflon density on temperature, make only very minor changes to these results.

The second evaluation used the simpler analytical integrated potential, no angular average, but was done with and without a Maxwellian energy distribution. The general results were the same with the spread in atomic energies reducing the temperature dependence by a factor of 3.

### C. Transfer of Energy during Collisions

Optical pumping experiments with evacuated coated

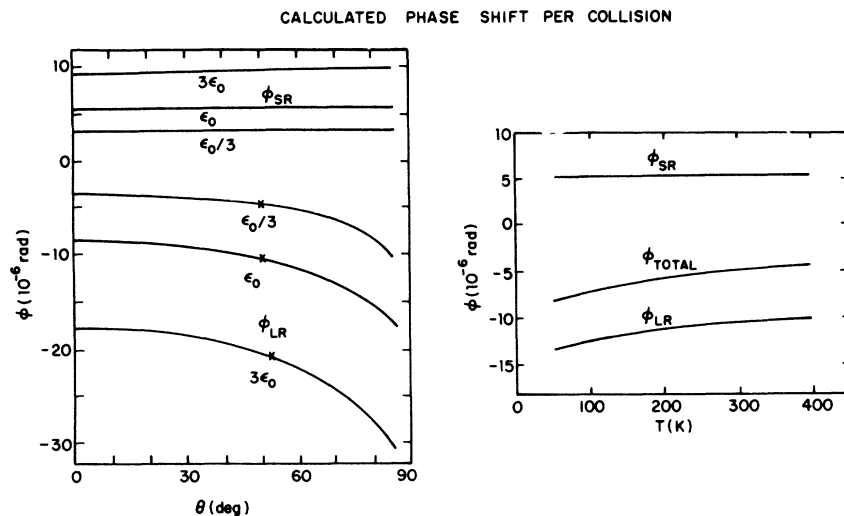


FIG. 1. Calculated phase shift per collision, (a) as a function of approach angle at 300°K and (b) averaged over the approach angle.

cells using rubidium<sup>30</sup> suggest that the atoms are physically adsorbed on the paraffin surfaces. Moreover, analysis of early wall-shift temperature-dependence measurements in the hydrogen maser suggested the same mechanism.<sup>3</sup> In order to examine this question thoroughly, three estimates must be made; first, the amount of energy lost per collision; second, the probability of trapping per collision; third, the length of time trapped and the resulting phase shift per collision.

Energy loss during a collision is commonly specified in either of two ways. The accommodation coefficient (AC)  $\alpha$  is usually defined<sup>31</sup> as

$$\alpha = (E_i - E_f)/(E_i - E_s) ,$$

where the subscripts  $i$ ,  $f$ , and  $s$ , refer to the initial and final atomic energies and to the surface atom energy, respectively. The alternative is the unit accommodation coefficient, or energy transfer coefficient (ETC)  $\alpha'$ , which is the AC for a zero temperature surface. Equivalently, the ETC is the proportion of kinetic energy lost by an atom in a collision. That is,  $\alpha' = (E_i - E_f)/E_i$ . A simple calculation of  $\alpha$  can be made<sup>31</sup> by assuming that the atom-surface interaction arises from hard-sphere repulsive forces with no attractive component. When this assumption is combined with the assumptions of zero surface temperature and of independent motions of the surface atoms, the result is  $\alpha = 4\mu/(1 + \mu)^2$ , where  $\mu$  is the ratio of masses of gaseous and surface atoms. In the present problem  $\mu = \frac{1}{19}$  and thus  $\alpha = 0.19$ . Several theories have been developed to relax these restrictions. The one of Karamcheti and Scott<sup>32</sup> uses a one-dimensional continuum to represent the surface. The resultant ETC is given by

$$\alpha' = H(kT_g/\epsilon)(\mu B)^{1/2} , \quad (7)$$

where  $T_g$  is the gas temperature,  $\epsilon$  the potential depth,  $H$  a function which is slowly varying for  $kT_g/\epsilon > 0.5$ , but which rises rapidly for arguments smaller than 0.5.  $B$  is the ratio of gas-surface to surface-surface interactions. Reasonable estimates of these parameters and also of the effective mass of surface groups involved give  $\alpha' = 0.07$  when the collision energy is transferred into the covalent bonds and 0.11 when it goes into the weaker inter-chain interactions. These estimates suggest that there is no difficulty in obtaining thermal equilibrium between surface and atoms during the  $\sim 10^5$  collisions made by the atoms. This conclusion is supported by some preliminary measurements.<sup>33</sup>

Dehmelt<sup>34</sup> has given general arguments for the probability of trapping at a surface. It was noted above that  $\alpha' = \Delta E/E$ ,  $E$  being the kinetic energy of the atoms. Thus the amount of energy lost by an atom in a collision with a surface having a potential well of depth  $\epsilon$  is  $\alpha'(E + \epsilon)$ . If this amount is larger than the original energy  $E$ , the atom is trapped. The finite temperature of the wall gives atoms a second chance to escape since the surface can as easily give energy to the atoms as take energy from them. Thus the final probability of trapping is

$$[(\epsilon/kT)(\alpha'/(1 - \alpha'))]^2 .$$

At 300°K in the maser the probability is  $7 \times 10^{-3}$ . This calculation suggests that trapping should be unimportant in the maser at this temperature.

For a simple square-well approximation to the atom-surface interaction with only one bound (physically adsorbed) state, the length of time an atom is trapped can be found from a phase-space calculation.<sup>29</sup> The result is  $t = t_0 e^{E_A/kT}$ , where  $t_0$  is the time required for the atom to cross the well once ( $\sim 10^{-12}$  sec) and  $E_A$  is the energy of the adsorbed state. The phase shift of the hydrogen hyperfine

suffered during such a collision is  $\phi_{sr} + \phi_{lr} e^{E_A/kT}$ , where the two phase shifts are those calculated above and where we have assumed that a trapped atom does not have sufficient energy to penetrate into the region of the short-range interaction. The total phase shift would be very negative at low temperatures and would be reduced asymptotically as the temperature is raised. A more realistic adsorption model has the atom and surface continually exchanging small amounts of energy and thus has the atom moving rapidly among many bound states. The phase shift is not given by a simple formula, but still could be expected to have a decreasing slope at high temperatures.

### III. EXPERIMENTAL EQUIPMENT AND MEASUREMENT TECHNIQUES

The experimental work was performed on a modified Varian H-10 hydrogen maser,<sup>2</sup> as shown in Fig. 2. The pumping capacity of the vacuum pumps was increased by changing the manifold to permit installation of an Orb-Ion-type electrostatic ion pump (Norton Corporation). Although this pump has not proved to be reliable under continuous heavy hydrogen loads, it has worked well when operated only intermittently at full power. The original 240 liter/sec Vac-Ion pump (Varian Corporation) pumping the bulb, or rf region maintains high vacuum ( $10^{-8}$

Torr) at all times. Other changes include a mechanical valve for the hydrogen gas rather than the Pd-Ag leak, a magnetic field-excited hydrogen discharge, and separate evacuation to fore-pressure of the cavity bell jar. The storage bulb is sealed to the rf region with a Viton O-ring, the only organic material in the high-vacuum region.

The major method of investigation of the wall shift has been the measurement of this shift over a wide range of temperatures. In the range from room temperature to 410 °K a conventional electrical heating system was used. A 30-W heater on the bell jar and a 250-W unit on a cylinder between the two magnetic shields, controlled by a system using thermistor sensing and continuous dc control, permitted regulation to within 0.1 °K. For experiments below room temperature a system was developed which allowed work between 100 and 300 °K. The bulb to be cooled is within a high-Q cavity in a region of high magnetic field homogeneity. In view of these constraints on cryogenic systems, it was decided to replace the normal quartz cavity with one made of copper with hollow side walls. The filling of these walls and an additional 8-liter capacity storage Dewar inside the bell jar with liquid nitrogen then provided the cooling for the bulb. Radiational cooling was aided by conduction via the residual air in the bell jar (500 Torr). The close proximity of the cavity to the bell jar (2 mm separation) together with the necessary connections to the cavity gave extensive heat leaks which prevented the temperature from reaching 77 °K. Temperature was measured by copper-constantan thermocouples on four places on the cavity with a weighted average providing the bulb temperature. The bulb temperature could differ from this average because of thermal time lags and heat leaks along the stem. The latter were eliminated by providing a heat sink from the quartz stem to the cavity bottom plate with copper wool.

In a typical operation the cavity and storage Dewar were filled with liquid nitrogen and the system pre-cooled for 90 min using about 30 liters of nitrogen. Measurements of the wall shift were then made near 100 °K for about 1 hr using an additional 5–10 liters. The liquid was allowed to evaporate completely and rapid measurements were made as the maser warmed up. One more fixed temperature point at 284 °K was made with cold water replacing the liquid nitrogen.

The quantity actually measured is the difference in frequency between the test maser and a reference maser. The method of making these measurements and the calibration of the reference has been described previously.<sup>13</sup> In brief, each wall-shift determination consists of a measurement of the cavity and spin-exchange pulling of each maser and a measurement of the two Zeeman frequencies needed for

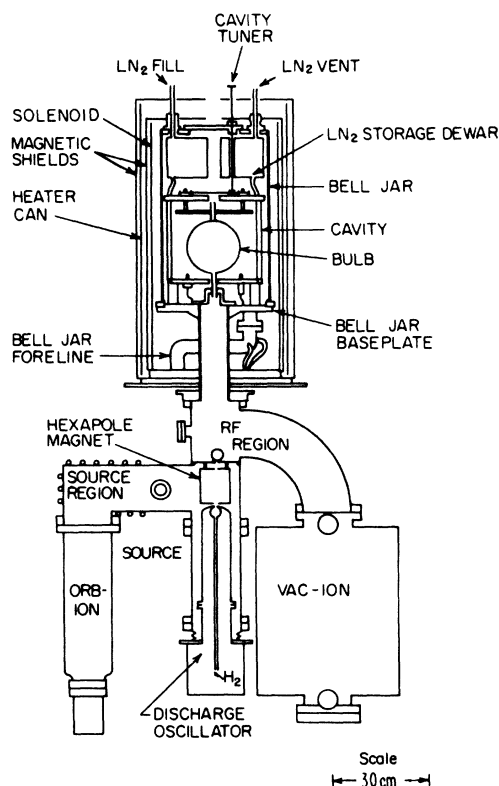


FIG. 2. Schematic diagram of hydrogen maser.

the magnetic field correction. In a typical wall-shift measurement, ten such determinations are made, with a scatter (standard deviation of the mean) of 0.2 mHz (1 mHz =  $10^{-3}$  Hz). One or two temperature measurements in order to correct for second-order Doppler shifts complete the measurement. The phase shift per collision  $\phi$  is calculated via  $\phi = 4\pi d\delta\nu_w/3\bar{v}$ , where  $d$  is the bulb diameter,  $\delta\nu_w$  the wall shift (including stem correction),<sup>13</sup> and  $\bar{v}$  the mean atomic velocity.

During the rapid warmup of the maser after the liquid nitrogen has evaporated, a different measurement technique is required. The cavity is changing frequency so quickly that the maser oscillates for only 3 min without retuning. The technique adopted is based on the linear dependence of cavity frequency on temperature and the assumed linear increase of temperature with time. The maser frequency is pulled by the cavity mistuning approximately linearly, with a factor of proportionality  $\Delta\nu_a/\Delta\nu_c$ , the ratio of atomic and cavity linewidths.<sup>4</sup> Thus it is expected that the maser frequency should change linearly with time, faster for larger atomic linewidths. By alternating high and low hydrogen fluxes, and thus wide and narrow linewidths, segments of two straight lines can be generated. Least-squares fits of the two and their intersection at the true maser frequency provide the wall-shift measurement. Scatter was about 3 mHz. Temperature measurements before and after each 3-min run, Zeeman determination, and reference maser checks complete the measurement.

#### IV. EXPERIMENTAL RESULTS

Measurements from room temperature to 410°K were made on two coatings of each type of Teflon. The FEP-120 work was done on two bulbs, one 10 cm in diameter, the other 16.4. The TFE-42 experiments involved separate coats on one 15.7-cm bulb. For one coat, the bulb lifetime, set by the natural stem of the bulb, was 0.4 sec. For the other, a quartz stem insert coated with TFE-42 was used to increase the lifetime to 3.2 sec. In all four cases the measurements were first made at low temperature, then various higher temperatures, finally low again. After each temperature change, 24 h were allowed for the bulb to reach equilibrium. When a FEP-120 bulb had been exposed to air for several weeks, the low-high-low temperature run did not converge at low temperatures. However, agreement with the wall shift at low temperatures before the exposure to air was obtained after baking out.

Below room temperature only one coating of each type of Teflon was measured. The phase shift between 295 and 315°K was first determined, next a run to 100°K was made, and then several to collect data between 130 and 250°K. Finally, the cold-water run was made near 280°K. Because of the

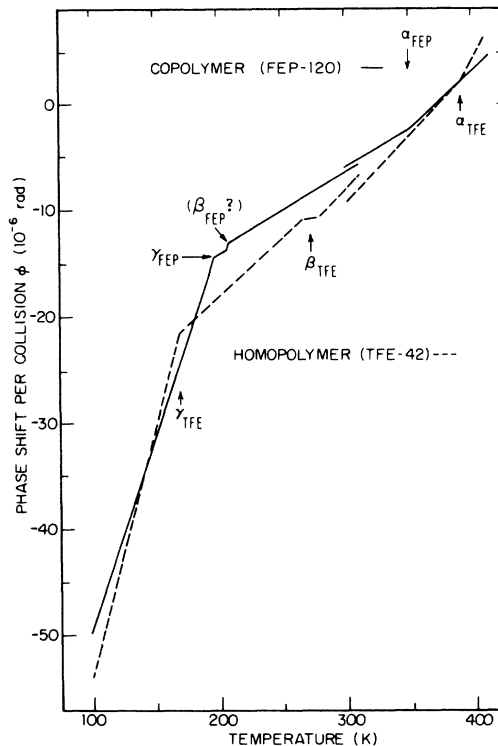


FIG. 3. Experimental phase shift per collision versus temperature.

lack of temperature homogeneity and the possible time lags, all temperatures between 100 and 250°K may be uncertain by  $\pm 5^\circ\text{K}$ .

The general results are shown in Fig. 3. There are three major points of interest. First, the slope is large, more than ten times that predicted by the theory; second, the phase shift passes through zero near 100°K for both materials, and the slope increases at higher temperatures; third, the phase shift is essentially linear with temperature in between abrupt changes.

It was first tried, without success, to fit  $\phi(T)$  by a power series. It was then found that piecewise linear functions gave excellent agreement and, by calling attention to the abrupt changes in  $\phi(T)$ , suggested the analysis of the results given in Sec. V.

The general program adopted was to fit  $\phi(T)$  to a function of the form  $AT + B$  by means of a statistically weighted linear least-squares fit (LLS) within restricted temperature regions. A plot was then made of the residuals, that is, the differences between the experimental points and the generated function. Further small adjustments were made by excluding from the fit all points in the transition regions between the linear segments. In three figures (see Figs. 4–6) details of these transitions are shown. In all three the temperature regions over which the fits were made are shown by solid lines,

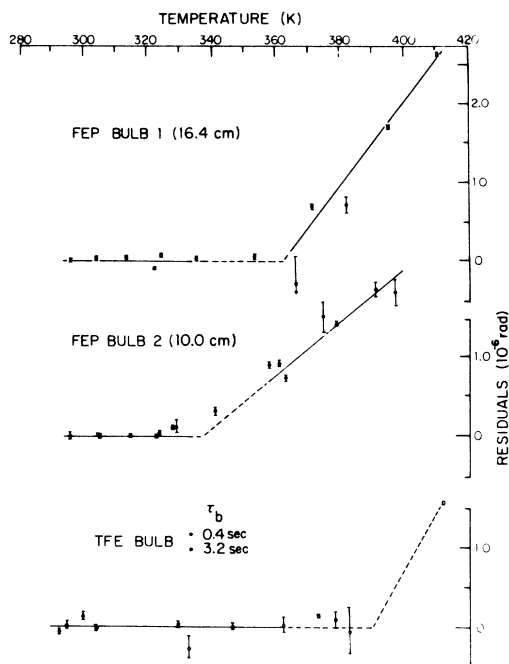


FIG. 4. Residuals from least-squares fits above room temperature.

the transition regions by dashed ones. Figure 4 shows the results of all the high temperature runs. The residuals from the LLS fit between 205 and 312 °K for the FEP-120 coating are shown in Fig. 5. The fit includes both the well-determined points in the room-temperature region and the less well-known data

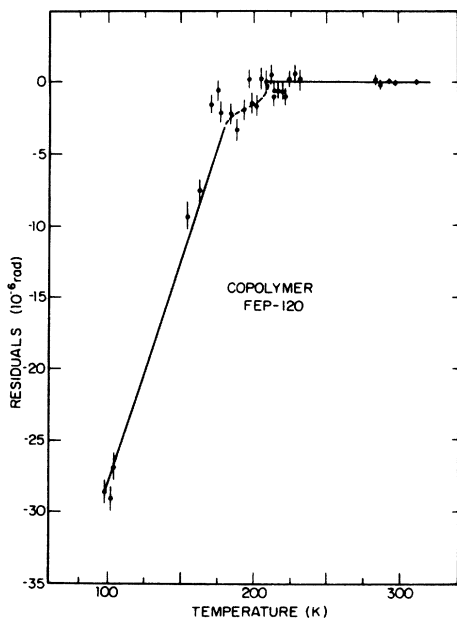


FIG. 5. Residuals from least-squares fits below room temperature, FEP-120.

below 250 °K. The solid line between 100 and 160 °K is the result of a second LLS fit in that region. The shoulder at the intersection is only a suggestion that will be discussed later. The TFE-42 results in Fig. 6 are residuals from a LLS fit between 180 and 255 °K. Here there is a definite discontinuity between these data and the room-temperature points. Again the lowest temperature data are fitted separately. The parameters for all these fits to  $\phi = AT + B$  are listed in Table I. Temperatures of the discontinuities, labeled  $\alpha$ ,  $\beta$ ,  $\gamma$  in order of decreasing temperature where  $\beta$  is a discontinuity in the phase shift and  $\alpha$  and  $\gamma$  are discontinuities in its slope, are given in Table II. Whenever two or more bulbs were measured over a given temperature range an average of the parameters is given.

#### V. DISCUSSION OF TEFLON RESULTS

There are three major experimental results that must be accounted for. First is the magnitude and slope of the phase shift. Second is the existence of the zero crossing. Third is the abrupt changes in slope. Comparisons of the experimental results with Fig. 1 show that the magnitude of the shift is consistent with theory, but the slope is much greater. No reasonable variation of the parameters in the present theory can provide the needed increase in slope. It is quite likely that the fault lies in the short-range hyperfine shift.<sup>35</sup> A hyperfine shift that varies more rapidly than the interaction potential should lead to a larger slope. Such a shift might be due to the many-body effects inherent in an atom-

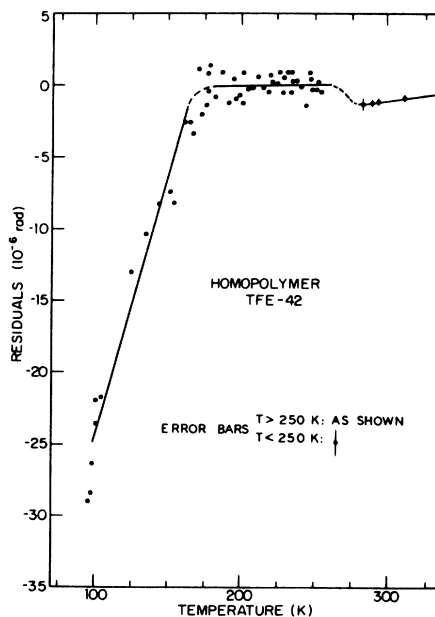


FIG. 6. Residuals from least-squares fits below room temperature, TFE-42.

surface problem which have been completely neglected in the present computation.

The zero crossing is best explained by the adiabatic collision model which sees the total phase shift as a balance between positive and negative components. A physical adsorption model would explain the temperature dependence as the result of the atom spending more time making many passes across the negative shift region at lower temperatures, and would finally come into agreement with the adiabatic model at high temperatures. However, this would require the phase shift due to a single pass over the well to be much smaller than present calculations show, and these calculations are the strongest part of the theory. Moreover, the small trapping probability estimates further increase the case against physical adsorption.

Besides the differences in the temperatures at which there are discontinuities in the phase shift or its slope, the major differences between the FEP-120 and TFE-42 data are the slope and magnitude of the phase shift near room temperature. Two suggestions for these differences can be made. First, the negative portion of the phase shift is sensitive to the density of interaction centers averaged over a relatively large volume, while the positive part, caused by a much shorter-range potential, is caused by only a few atoms, and thus less sensitive to macroscopic, or total, density. Physically, the difference between the two Teflons is the smaller rigidity of the copolymer primarily due to the weakening of the interchain forces by the comonomers. Thus in the copolymer the total density is smaller although the chain density is higher. This suggests that the negative part of the phase shift would be smaller for the copolymer, and thus that the total phase shift would be more positive, as observed. Second, if the surface is not perfectly smooth, the calculation of the phase shift per collision from the wall shift would give too large a result. This would mean that added surface roughness would rotate the phase shift versus temperature line about its zero crossing. Since it has been noted that homopolymer coats appear rough, some of the excess wall shift

TABLE I. Parameters for the piecewise linear fits of phase shift per collision versus temperature,  $\phi = AT + B$ .

Coating	Temperature range (°K)	A ( $\mu\text{rad}/^\circ\text{K}$ )	B ( $\mu\text{rad}$ )
TFE-42	100-165	0.468	-100.4
	170-250	0.111	-40.4
	285-380	0.127	-47.4
	400-412	$\sim 0.2$	$\sim -84$
FEP-120	100-165	0.413	-90.6
	200-330	0.069	-26.9
	360-410	0.109	-40.8

TABLE II. Approximate temperatures (°K) for discontinuities in the phase shift per collision or its slope.

Coating	$\alpha$	$\beta$	$\gamma$
TFE-42	385-405	260-280	165-175
FEP-120	335-360	200(?)	175-185

at room temperature might be due to this effect.

There are three well-known phase changes in Teflon, each with an associated molecular relaxation.<sup>16</sup> Experimentally, peaks are observed in the electromagnetic and mechanical loss spectra, with the frequency of the peaks depending on sample temperature. The frequency-temperature relation is that given by the law of chemical activation

$$f = (kT/2\pi h) e^{-\Delta E^\ddagger/kT},$$

where  $\Delta E^\ddagger$  is the free energy of the activated process. These processes are interpreted as the onset of motion of groups of atoms in the chains. In Fig. 7 the temperature-frequency curves are shown for the homo- and copolymer, together with the discontinuity temperatures for the phase-shift data. There is excellent agreement for the five relaxations for which there are polymer data. The frequency  $10^{-2}$  Hz suggested here should not be given too much weight, as there is no experimental polymer data below  $10^{-1}$  Hz and there is some theoretic-

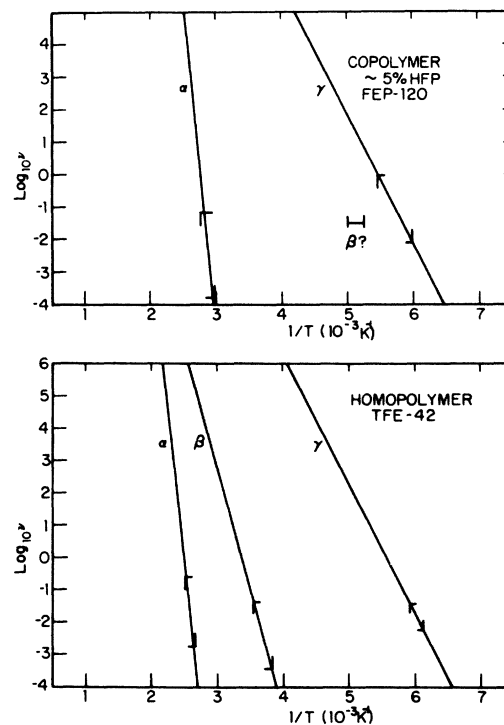


FIG. 7. Polymer relaxations and the abrupt changes in the phase shift.

cal reason to believe that the chemical activation model is inaccurate at very low frequencies.

This correlation between wall shift and surface properties is the first indication that there is a direct connection, although it is difficult to find a one-to-one correspondence between the physical processes occurring in the bulk polymer and the observed wall-shift changes. There are some hints, though. At the  $\alpha$  relaxation large segments of the molecular chains begin to move. This occurs at lower temperatures in the copolymers. This motion would be fast enough to reduce the long-range attraction by a type of motional averaging, but not fast enough to affect the short-range interaction, so the result would be a more positive phase shift, as observed. The  $\beta$  relaxation is associated with the complex chain and crystal transformations near room temperature.<sup>10</sup> These transformations at 19 and 30 °C in the homopolymer, however, are not observed. Both polymer and phase-shift changes are complex. The  $\gamma$  relaxation in the polymers is associated with the primary glass transition. Above this temperature the material is a plastic; below, its properties are more glasslike. It is possible that below this temperature the combination of stronger interchain bonding and the increase in energy loss per collision caused by the increase in  $H$  in Eq. (7) combine to make physical adsorption important here. More experimental data are needed, especially at the low-temperature end, before a decision can be made. It is not necessary for hydrogen to be physically adsorbed, as the wall could be changed by adsorbed impurities below this temperature.

#### VI. ADDITIONAL SURFACE MATERIALS

Two other surfaces have been investigated briefly. One, Drifilm, has long been used in masers. The wall shift of a single sample was measured between 300 and 380 °K, giving a phase shift per collision of  $\phi = (-0.085 T - 50.9) \mu\text{rad}$ . The negative slope cannot be explained in terms of the kinematic effects of the theory present here, but it is possible to suggest a cause in terms of the surface structure. In the reaction of dimethyldichlorosilane with a silica surface, the chlorine reacts with the silica and is released to make the final result a surface of  $-\text{CH}_3$  groups bonded to silicon atoms. The hydrogen atoms do not provide the protective sheath given by the fluorine atoms in Teflon, and it is possible that at higher temperatures the gaseous hydrogen

atoms penetrate into the carbon and silicon potentials, suffering a larger negative phase shift.

The second surface tried was a film of a viscous liquid, Fluorolube,<sup>36</sup> a mixture of fluorinated hydrocarbons with a mean molecular formula  $\text{C}_{21}\text{H}_{44}$ . Coatings were prepared on 10 and 16-cm diameter bulbs. At room temperature (24 °C) the two wall shifts agree with those of FEP-120 Teflon. At 32 °C, however, they are substantially more negative. Moreover, the larger bulb is much more negative than the smaller one. At this temperature the vapor pressure is high enough ( $\geq 1 \times 10^{-5}$  Torr) so that gas-phase collisions become important. However, the excess negative phase shift cannot be interpreted as being due to gas-phase collisions unless the phase shift per gas collision is larger (more negative) than that of a surface collision. This is unlikely. Because of the excessive vapor pressure, which created a larger load on the vacuum pumps, no further measurements were made. The equality of the room-temperature phase shifts with those of Teflon does seem further to support the conclusion that the wall shift observed with Teflon is primarily a result of the surface material itself and not due to impurities in the vacuum system or in the material.

#### VII. CONCLUSIONS

We have examined the frequency shifts in the hydrogen maser due to surface collisions. Measurements of the temperature dependence tend to support the model of an adiabatic collision, although the present theory does not adequately explain the data. Inadequacies in the model suggest where further theoretical work might be done. The wall shift passes smoothly through zero near 100 °C, which may have important applications in the use of the maser as a frequency standard.<sup>37</sup> Finally, the identification of abrupt changes in the temperature dependence of the phase shift with relaxations associated with phase changes in Teflon has provided a direct connection between the wall shift and surface properties. Thus the hydrogen maser can be used as an experimental tool to study atom-surface interactions, albeit indirectly.

#### ACKNOWLEDGMENTS

We wish to thank Professor H. C. Berg, Professor S. B. Crampton, and Dr. R. F. C. Vessot for many useful discussions.

\*Work supported by the National Aeronautics and Space Administration and the National Science Foundation.

†Work based on a dissertation presented by one of us (P. W. Z.) to Harvard University in partial fulfillment of the requirements for the degree of Doctor of Philosophy in Physics.

‡Danforth Graduate Fellow during course of this work. Present address: University of Western Ontario, London, Ontario, Canada.

<sup>1</sup>D. Kleppner, H. M. Goldenberg, and N. F. Ramsey, *Phys. Rev.* **126**, 603 (1962).

<sup>2</sup>D. Kleppner *et al.*, *Phys. Rev.* **138**, A972 (1965).

- <sup>3</sup>H. C. Berg, *Phys. Rev.* **137**, A1621 (1965).  
<sup>4</sup>S. B. Crampton, *Phys. Rev.* **158**, 57 (1967).  
<sup>5</sup>S. Ray, J. D. Lyons, and T. P. Das, *Phys. Rev.* **174**, 104 (1968).  
<sup>6</sup>H. Hellwig, R. F. C. Vessot, M. Levine, P. W. Zitzewitz, D. Allen, and D. Glaze, *IEEE Trans. Instr. Meas.* (to be published).  
<sup>7</sup>Preliminary results published in P. W. Zitzewitz and N. F. Ramsey, *Bull. Am. Phys. Soc.* **14**, 943 (1969); **15**, 46 (1970); and P. W. Zitzewitz, in *Proceedings of the Twenty-Fourth Annual Frequency Control Symposium*, Atlantic City, New Jersey, 1970 (unpublished).  
<sup>8</sup>This would be true for chemically pure fluorocarbons, but not for Teflon; see Ref. 3.  
<sup>9</sup>T. M. Reed, III, in *Fluorine Chemistry*, edited by J. H. Simons (Academic, New York, 1964).  
<sup>10</sup>For a general review, see C. A. Sperati and H. W. Starkweather, Jr., *Fortschr. Hochpolymer-Forsch.* **2**, 465 (1961).  
<sup>11</sup>P. H. Geil, *Polymer Single Crystals* (Interscience, New York, 1963).  
<sup>12</sup>A. Keller, *Phys. Today* **23**, 42 (1970).  
<sup>13</sup>P. W. Zitzewitz, E. E. Uzgiris, and N. F. Ramsey, *Rev. Sci. Instr.* **41**, 81 (1970).  
<sup>14</sup>R. Vessot, P. W. Zitzewitz, and H. Hellwig (unpublished).  
<sup>15</sup>M. I. Bro and C. A. Sperati, *J. Polymer Sci.* **38**, 289 (1959).  
<sup>16</sup>R. K. Eby and F. C. Wilson, *J. Appl. Phys.* **33**, 2951 (1962).  
<sup>17</sup>M. I. Bank and S. Krimm, *J. Appl. Phys.* **40**, 4248 (1969).  
<sup>18</sup>J. F. Lontz and W. B. Happoldt, Jr., *Ind. Eng. Chem.* **44**, 1800 (1952).  
<sup>19</sup>N. F. Ramsey, *Molecular Beams* (Oxford U. P., London, 1956).  
<sup>20</sup>W. Brandt, *J. Chem. Phys.* **26**, 262 (1957).  
<sup>21</sup>J. O. Hirschfelder, C. F. Curtis, and R. B. Bird, *Molecular Theory of Gases and Liquids* (Wiley, New York, 1954).  
<sup>22</sup>J. N. Wilson, *J. Chem. Phys.* **43**, 2564 (1965).  
<sup>23</sup>A. Dalgarno and W. D. Davison, in *Advances in Atomic and Molecular Physics*, edited by D. R. Bates and I. Estermann (Academic, New York, 1966), Vol. II.  
<sup>24</sup>W. D. Davison, *J. Phys. B* **2**, 1110 (1969).  
<sup>25</sup>G. A. Clarke, *J. Chem. Phys.* **36**, 2211 (1961).  
<sup>26</sup>J. H. Wright, L. C. Balling, and R. H. Lambert, *Phys. Rev. A* **1**, 1018 (1970).  
<sup>27</sup>F. J. Adrian, *J. Chem. Phys.* **32**, 972 (1960).  
<sup>28</sup>Y.-H. Pao and R. J. Bjorklund, *J. Appl. Phys.* **31**, 1925 (1960).  
<sup>29</sup>J. H. DeBoer, in *Advances in Colloid Science* (Interscience, New York, 1950).  
<sup>30</sup>R. G. Brewer, *J. Chem. Phys.* **38**, 3015 (1963).  
<sup>31</sup>D. M. Gilbey, *J. Phys. Chem. Solids* **23**, 1453 (1962).  
<sup>32</sup>K. Karamcheti and L. B. Scott, Jr., *J. Chem. Phys.* **50**, 2364 (1969).  
<sup>33</sup>H. E. Peters (private communication).  
<sup>34</sup>H. G. Dehmelt, in *Proceedings of the Twenty-Fourth Annual Symposium on Frequency Control*, Atlantic City, New Jersey, 1958 (unpublished).  
<sup>35</sup>This also seems to be the case for the calculation of the pressure shift in optical pumping. There the slope is correct for D-He but the magnitude is wrong. See Ref. 25.  
<sup>36</sup>Courtesy of Dr. K. Rapp, Oak Ridge National Laboratory.  
<sup>37</sup>R. F. C. Vessot and M. W. Levine, in *Proceedings of the Twenty-Fourth Annual Symposium on Frequency Control*, Atlantic City, New Jersey, 1970 (unpublished).

## Detection of Positronium Hydride\*

David M. Schrader and Teri Petersen

*Chemistry Department, Marquette University, Milwaukee, Wisconsin 53233*

(Received 16 February 1970)

Annihilation converts positronium hydride into photons and a hydrogen atom. We calculate the probability that the residual hydrogen atom will relax to each of number of bound states. The results suggest an experiment for detecting positronium hydride in a system in which excited hydrogen atoms do not exist except as the residue after annihilation. The experiment consists of measuring the intensity increase of the Lyman- $\alpha$  line upon quenching the 2s atoms to 2p atoms. We predict that the intensity will increase by a factor of 35.

### INTRODUCTION

For annihilation in molecular media, identification of the parent (i. e., the positron plus atom or molecule) is an important part of deducing the mechanism for the annihilation process and for relating angular-correlation data to structure. Except for positronium (Ps) itself, lifetime and angular-correlation data do not yet provide an unambiguous

means for identifying the parent. We present here a method of identification which does not rely on these data, but rather on the relaxation of the daughter (residue after annihilation).

We assume that the annihilation event takes place instantaneously, that it involves only the annihilating pair, and that the spectator electrons do not begin to relax into eigenstates of the new Hamiltonian until after annihilation is finished. Chang Lee<sup>1</sup>